

Radioactive Analysis of Magneto hydrodynamic (MHD) Micro-pump

Submitted By

Abyaz Abid

180011137

Supervised By

Dr. Arafat Ahmed Bhuiyan

Co-Supervised By

Abul Kalam Azad

**A Thesis submitted in partial fulfillment of the requirement for the degree of Bachelor of
Science in Mechanical Engineering**



Department of Mechanical and Production Engineering (MPE)

Islamic University of Technology (IUT)

19th May, 2023

Candidate's Declaration

This is to certify that the work presented in this thesis, titled, “**Radioactive analysis of Magneto hydrodynamic Micro pump**”, is the outcome of the investigation and research carried out by me under the supervision of **Dr. Arafat Ahmed Bhuiyan**.

It is also declared that neither this thesis nor any part of it has been submitted elsewhere for the award of any degree or diploma.

Abyaz Abid

Name of the Student

Student No: **180011137**

RECOMMENDATION OF THE BOARD OF SUPERVISORS

The thesis titled “**Radioactive analysis of Magneto hydrodynamic Micro pump**” submitted by **Abyaz Abid**, Student No: **180011137** has been accepted as satisfactory in partial fulfillment of the requirements for the degree of B Sc. in Mechanical Engineering on **18th May, 2023**.

BOARD OF EXAMINERS

1. -----

Dr. Arafat Ahmed Bhuiyan

(Supervisor)

Associate Professor

MPE Dept., IUT, Board Bazar, Gazipur-1704, Bangladesh.

2. -----

Abul Kalam Azad

(Co-Supervisor)

Assistant Professor

MPE Dept., IUT, Board Bazar, Gazipur-1704, Bangladesh.

Abstract

This study aims to investigate blood-based hybrid nanofluids in a Magneto-hydrodynamic (MHD) micropump for biomedical applications. The study examines three blood-based bio-convective radiating hybrid nanofluids (Ti₂O, Cu₂O, and Ag) and analyzes the influence of fluid, magnetic, and electrical properties on the radiation characteristics of the MHD micropump using dimensionless parameters (R_d and R_e). Results indicate that Ti₂O nanofluid exhibits efficient radiative behavior, affecting velocity distribution in the micropump channel. Cu₂O and Ti₂O nanofluids show minimal pressure drop during high radioactivity, ensuring smooth blood flow in microscale intravenous (IV) treatment. Ti₂O shows high magnetic flux density for effective blood pumping, although increased radiation generation raises concerns for general IV treatment. Cu₂O exhibits desirable electrical flux intensity, suitable for low radiative therapy. The study concludes that Ti₂O nanofluid is most effective for blood-based intravenous treatments with potential applications in various therapeutic interventions requiring superior nanoparticle properties.

Contents

1. Abstract	4
2. Introduction	5
3. Domain Setup	8-10
4. Governing equations	10-11
5. Boundary Conditions	11-12
6. Dimensional Analysis	12-13
7. Nanofluid Properties	13-14
8. Mesh generation and convergency test	14-15
9. Validation	15-16
10. Result and Discussion	16-24
11. Conclusion	24-25
12. Conflict of interest	25
13. Reference	26-30
14. Turnitin Report	31

Introduction

The concept of “Magnetohydrodynamic” (MHD) is simply a beyond phenomenon of two established disciplines – fluid mechanics and magnetic effect – when the velocity field and magnetic field coupled each other for any electrically conducting fluid through a solid body with motion. The fundamental of MHD activity is the combination of electrical force and magnetic force to produce non-mechanical thrust or pressure gradient by the virtue of Lorentz force in order to transfer transport fluid particles [1]. Over the past 20 to 30 years different applications of such fluid flow have been developed and researched intensively. Material processing and other metallurgical process of steel, aluminum and various superalloys are revolutionized by magnetohydrodynamic (MHD) [2]. Interaction between thermal and magnetohydrodynamic field owes to a new type of domain termed as Thermoelectric magnetohydrodynamic which deals with the Peltier and Thomson effect to solve *ab initio* problems as well as to stir and pump liquid-metal coolant in nuclear reactors. Another success of MHD implantation is the MHD power generators which proves to be zero pollution power generation system with efficiency surpassing the conventional generators by 20-35%. Incorporating MHD effect in different kinds of microfluidics devices and systems such as – MHD pump, propelling and stirring liquid, assessing blood network and MRI are some of the most popular applications [3]–[5]. Extensive study has already been done and still ongoing to understand the applicability of nanofluids combined with MHD effect in different porous cavities, double diffusive convection, parallel flow medium and various application-based domain [6], [7].

One of the most widespread and variable application of MHD based fluid flow system is the Magneto-Hydrodynamic Micro Pump. Most common yet impactful applications of such MHD micropump in recent times are – micro-macro total analysis of blood analysis technology (μ – TAS) [8]–[10]. Driving force of a MHD micropump is the Lorentz force developed perpendicularly with both the electric and magnetic field which themselves are applied at square of each other. Due to this force pressure gradient is created which forces blood to transport from inlet (source/high pressure area) to outlet (destination/low pressure area) without any mechanical actuation [11]–[13]. Numerous studies covering both the experimental and computational arenas, show progress of MHD micropump for total analysis of blood technology over the years [11], [12]. Inspection of fully developed viscous flow of Newtonian bio magnetic fluid such as – blood under the influence of varying ferro hydromagnetic and magnetohydrodynamic effect has been done by E.E. Tzirtzilkakis in [16]. A new type of blood flow model termed as “Jeffery blood model” has been introduced by M.M.Bhatti and et al. in which blood is passed through a porous channel of MHD pump [17]. The outcomes showed that the velocity and pressure of the blood flow rises near the wall due to slip effect of the creeping regime. A similar methodology has been applied in order to simulate in a new type blood flow model termed as Casson flow through MHD micro pump by neglecting the inertial forces [18]. The results are plotted concentrating specially to the heat and mass transfer process through the MHD micropump along with the impact of magnetic and electrical field on related velocity and pressure profile. Interesting figures were found as the velocity profile exhibited contrasting attribute compared to pressure profile due the emergence of peristaltic wave.

Bio-rheological non-Newtonian liquid such as – blood-based hybrid nano fluid are proved to be effective transport medium for drug delivery, blood transport through veins and many biomedical applications due to their potential thermal features, increased rate of heat transport, mechanical stability etc [19]–[24]. Hydrothermal features of an incompressible, unsteady and laminar flow of hybrid blood based nanofluid (GO + ZnO + Blood) are studied analytically which explored pertinent physical parameters with respect to varying strength of magnetic field, electric flux intensity etc [25]. Pulsatile CuO – Fe₃O₄ blood based nanofluid is inspected under a body of acceleration in order to understand its effectivity in radiation therapy of lung cancer. Study showed that this hybrid nanoparticle provides better thermal performance, opposite characteristics between velocity and body force parameter and higher blood flow compared to normal blood [26]. A secured mathematical framework is developed for a tri-hybrid nanofluid (CuO-TiO₂-Al₂O₃) in order to investigate its performance with respect to thermal radiation, energy emission, Ohmic heat, viscous dissipation etc [27]. Conclusion of the study shows that thermal radiation increases with the increase of magnetic strength while EMDH simulation estimated substantial impact of such nanofluid on magnetized drug delivery, hyperthermia therapy, magnetizer endoscopy and blood stream knowledge.

Compound nanofluids have recently been incorporated into medical technology to cancel cells or to provide therapeutic agents for deceased cells [28]–[31]. Alternatively, many mixed amalgamated blood based nanofluids are being used as the transport medium as well as the radiating agent to destroy cancer cells of human body within a very limited range [32]–[34]. Among recent experiments, one based on EMHD (electromagnetohydrodynamic) and thermal radiation case shows that the usual radiating nanofluids when mixed with bloods can exhibit non-linear thermal radiation and the attributes vary according to the particle sizes, shapes, amount in the base fluid etc [35]. Investigation of such radiation effect of industrial water based nanofluids has been carried out by Zahir Shah et al. to comprehend the influence of flow, magnetic characteristics on thermal radiation containing ferrous and graphene oxide particles for various industrial building such as – ships, chemical devices, electronic devices and medical plants. The outcome of such computational work provides a contrasting strata between velocity profile and thermal field [36]. A completely novel numerical method – Spectral Relaxation Method (SRM) under the opportunity of Cattaneo-Christov model theory has been developed to understand the behavioral change of blood-based hybrid nanofluids when they are allowed to pass through a stretchable area. While conducting particular focus was provided to the thermal radiation effect of the nanofluids which conduces outcomes into greater electrical field enhances both velocity and temperature profile whereas opposite is seen for increased Pr number [37]. Similar yet relatively new research of radiative heat transfer of such blood-based hybrid nanofluids transporting under MHD flow has been carried out for different applicable small scaled domains, such as – rotating thin disc, stretchable cylinder, moving heat source and sink, non-uniform heat flux, vertical porous flat plate etc [38]–[40].

Although a lot of scientific contribution has been provided to radiative characteristics of different nanofluids, MHD flow through various medium, feasibility of micropump for biomedical applications and so on; however, a comprehensive demonstration of radioactive impact analysis of such blood-based hybrid nanofluids within the domain of MHD micropump still lacks in available

literature. And therefore, the proposed paper seeks to explore this research gap and signifies the outcome as contribution to the field of biomedical engineering for transporting blood and delivering drug in human body. In order to inspecting the radiation behavior of MHD pump three different blood-based bio-convective radiating hybrid nanofluids are used as transport medium – $BL+Ti_2O$ (Titanium oxide nanoparticles), $BL+Cu_2O$ (Cuprous oxide nanoparticles) and $BL+Ag$ (Silver nanoparticles). Due to their self-radiating nature, the blood based nanofluids are coupled with an external heat source (Cu) and heat sink (Al) to protean and amplify the outcome of the computational study. Two dimensionless parameters Rd (Radiation number) and Re (Reynolds number) are introduced in this paper in order to present the outcomes under the scope of three fundamental criteria – fluid properties, magnetic properties and electrical properties of the MHD micropump. To observe the deviation of fluid properties such as – temperature gradient, velocity distribution and pressure drop along the flow channel of the MHD pump, the dimensionless numbers are considered within the range from one to five for Ra number. The other two rudimentary properties – magnetic flux density (MFD) and electric flux intensity (EFI) are also being showed within the given range to understand how the nanoparticles behave inside human body during drug delivery and blood transportation.

Methods

Domain Setup

A conceptual schematic of Magneto Hydrodynamic (MHD) Micropump has been provided in **Fig. 1** The pump which is simply a combination of magnetic field, electric field and fluid transporting channel works based on the generated Lorentz force. The illustration provides directional guidance for the working MHD pump which has fluid flow, magnetic flux density and electric field intensity along x , z and y -direction respectively. The developed Lorentz force due to orthogonally applied electrical and magnetic force thrusts the fluid through the pump channel without any mechanical intervene. **Fig. 2 (a)** provides a complete set up for an experimental MHD micropump and **Fig. 2 (b)** displays an exploded view of the same pump. The pump is mainly consisting of three distinct layers – the lower layer holds magnetic source (in this case the Neodymium solid magnet) while the middle layer holds the fluid transport path of the pump. The upper most layer is the layer which protects the pump channel with a transparent glass cover and facilitates pressure measurement by holding two pressure measuring holes. There are also one inlet port for allowing the fluid into the pump and an outlet port to discharge the volume flow. Finally, **Fig. 3** captures a cross sectional view of the same MHD micropump to demonstrate the parts at micro level – a guide plate to separate out the magnet source (at lower layer) and acrylic plastic base (at middle layer), a thin copper film as grounding for setting series of copper micro electrode and finally an external voltage to provide just enough amount of current for the pump to work. A transparent glass cover is to protect the core flow channel of the pump from any external harm without disallowing outer supervision.

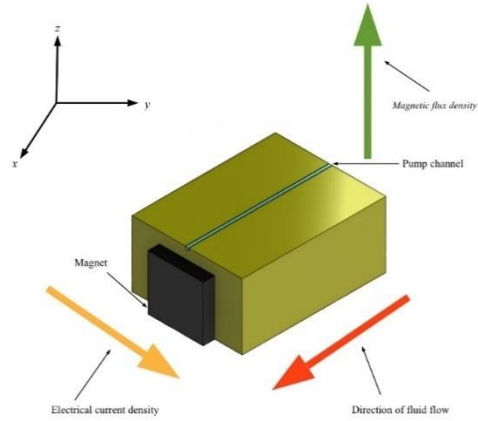
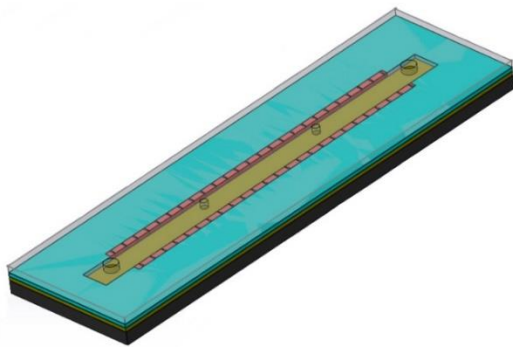
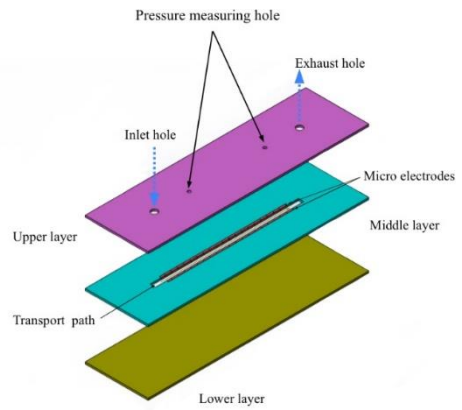


Fig. A conceptual design of the proposed MHD micropump.



(a)



(b)

Fig. Isometric view of the distinguished parts of the MHD micropump – (a) A full setup, (b) Exploded view of the setup.

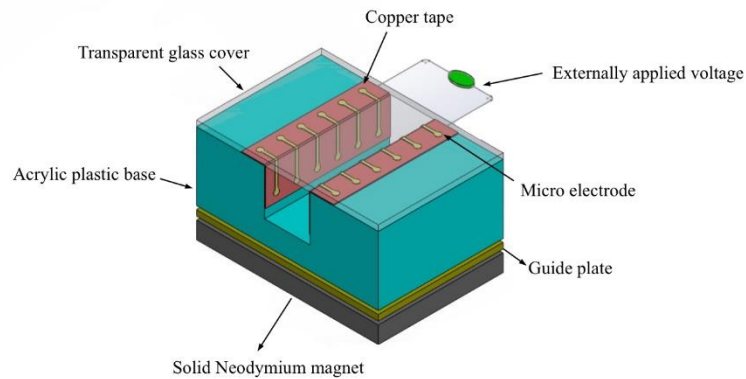


Fig. Cross sectional view of the MHD micropump.

Governing equations

Backbone of the applied mathematical modelling forums can be divided into three different categories – 1. Equations of electromagnetic system, 2. Conventional fluid dynamic system equations, 3. Thermal system of equations.

3.2.1 Equations of electromagnetic system

The electromagnetic system of the applied MHD micropump domain is contributed by three parameters – current density, magnetic flux density and electric field. Although allowing electrical conductance through the micropump channel induced magnetic effect on the overall geometry however, that effect is neglected due to negligible value of the associated magnetic Reynolds number R_{em} as abundantly found in available literature.

Maxwell equations:

$$\nabla \cdot D = \rho \quad (1)$$

$$\nabla \cdot B = 0 \quad (2)$$

$$\nabla \times E = -\frac{\partial B}{\partial t} \quad (3)$$

$$\nabla \times H = J + \frac{\partial D}{\partial t} \quad (4)$$

Ohm's Law:

$$J = \delta(E + u \times B) = \delta(-\nabla\phi + u \times B) \quad (5)$$

By combining with Ohm's Law:

$$J = \delta(E + v \times B) \quad (6)$$

The Lorentz force:

$$F_L = (J \times B) \quad (7)$$

3.2.2 Conventional fluid dynamic system equation

Fluidic part of the modelling system is consisting of simple continuity equation, momentum equation and energy equations.

Continuity equation:

$$\frac{\partial u}{\partial x} + \frac{\partial v}{\partial y} = 0 \quad (8)$$

Momentum equations:

$$\frac{\partial u}{\partial t} + u \frac{\partial u}{\partial x} + v \frac{\partial u}{\partial y} = -\frac{1}{\rho_{nf}} \frac{\partial p}{\partial x} + \frac{\mu_{nf}}{\rho_{nf}} \left(\frac{\partial^2 u}{\partial x^2} + \frac{\partial^2 u}{\partial y^2} \right) \quad (9)$$

$$\frac{\partial v}{\partial t} + u \frac{\partial v}{\partial x} + v \frac{\partial v}{\partial y} = -\frac{1}{\rho_{nf}} \frac{\partial p}{\partial x} + \frac{\mu_{nf}}{\rho_{nf}} \left(\frac{\partial^2 v}{\partial x^2} + \frac{\partial^2 v}{\partial y^2} \right) + \frac{\sigma_{nf} B_0^2}{\rho_{nf}} v + \frac{(\rho\beta)_{nf}}{\rho_{nf}} g(T - T_c) \quad (10)$$

Energy equations:

$$\frac{\partial T}{\partial t} + u \frac{\partial T}{\partial x} + v \frac{\partial T}{\partial y} = \alpha_{nf} \left(\frac{\partial^2 T}{\partial x^2} + \frac{\partial^2 T}{\partial y^2} \right) - \frac{1}{(\rho c_p)_{nf}} \frac{\partial q_R}{\partial y} \quad (11)$$

3.2.3 Thermal system of equations

The thermal energy equation is presented is below here:

$$\rho c \left(\frac{dT}{dt} + \mu \nabla T \right) = K \nabla^2 T + \frac{|J|^2}{\delta} \quad (12)$$

Thermal system of the domain is related due to flow of electric current through incorporated fluid medium used in the MHD micropump.

Boundary conditions

Similar to the governing equations of the modelling system boundary conditions are applied for implementing the basic fluid flow through the domain as well as interaction of electricity, magnetic and heat system with the pump's wall. The boundary conditions for the fluid-pump interaction are provided below.

3.3.1. Boundary conditions for fluid-pump interaction

Inlet boundary conditions

$$\frac{\partial u_{x,in}}{\partial x} = u_{z,in} = u_{y,in} = 0 \quad (13)$$

$$P_{in} = 0 \quad (14)$$

$$T_{in} = T_0 \quad (15)$$

Wall boundary conditions

$$u_{wall} = 0 \quad (16)$$

$$\frac{\partial P_{wall}}{\partial n} = 0 \quad (17)$$

$$T_{wall} = T_0 \quad (18)$$

$$\frac{\partial \varphi}{\partial n_{wall}} = 0 \quad (19)$$

Outlet boundary conditions

$$\frac{\partial u_{out}}{\partial t} + u_{x,out} \frac{\partial u_{out}}{\partial x} = 0 \quad (20)$$

$$P_{out} = 0 \quad (21)$$

$$\frac{\partial T_{out}}{\partial x} = 0 \quad (22)$$

$$\frac{\partial \varphi}{\partial n_{out}} = 0 \quad (23)$$

Electrode surface boundary conditions

$$\varphi_{anode} = V_{input} \quad (24)$$

$$\varphi_{cathode} = 0 \quad (25)$$

3.3.2. Boundary conditions for basic fluid flow through MHD pump

For $t = 0$: $u = v = 0, T = 0, p = 0$

For $t > 0$: $u = v = 0, T = T_h$ at $y = 0, 0.25L \leq x \leq 0.75L$

$u = u_0, v = 0, T = T_c$ at $y = L; 0 \leq x \leq L$

$u = v = 0, \frac{\partial T}{\partial N} = 0$ at $x = 0, L; 0 \leq y \leq L$

$u = v = 0, \frac{\partial T}{\partial N} = 0$ at $y = 0, 0 \leq x \leq 0.25L, 0.75L \leq x \leq L$

3.3.3. Jeffery- Hammel boundary conditions

Another fascinating aspect of the computational work is inspection of the impact of contraction-extraction of channel shapes when the blood-based hybrid nanofluids pass through different arteries and veins of human body. To realize such effect through the MHD pump a “close to” numerical output is harbored using Jeffery-Hamel dimensional analysis which is the direct implementation of Tiwari-Das nanofluid method [41].

$$\left\{ \begin{array}{l} \frac{\partial u}{\partial \theta} = 0, \frac{\partial T}{\partial \theta} = 0, u = U \\ u = -N_1 v_{nf} \frac{\partial u}{\partial \theta}, T = \frac{T_w}{r^2} - D_1 \frac{\partial T}{\partial \theta} \end{array} \right\} \begin{array}{l} \text{at } \theta = 0 \\ \text{at } \theta = \alpha \end{array} \quad (26)$$

Dimensional analysis

Following variables are converted into non-dimensional form in order to reduce the number of available variables and also to make the governing equations into non-dimensional simplified form. Non-dimensionalization is done for both the basic fluid flow and Jeffery-Hamel flow variables provided below respectively.

$$Y = \frac{y}{L}, X = \frac{x}{L}, U = \frac{u}{u_0}, V = \frac{v}{u_0}, P = \frac{p}{\rho_{nf} u_0^2}, \theta = \frac{T - T_c}{T_h - T_c} \quad (35)$$

$$\eta = \frac{\theta}{\alpha}, f(\theta) = ru(r, \theta), \Theta(\eta) = r^2 \frac{T}{T_w} \quad (36)$$

Nanofluid properties

As per the earlier mention, four different blood-based hybrid nanofluids have been used as the fluid medium for the micropump. To include the different fluidic properties such as – specific heat (C_p), viscosity (μ_{static}), effective density (ρ_{nf}), thermal expansion coefficient β_{nf} and thermal diffusivity (α_{nf}) of these nanofluids into the modelling system formulas are used and provided [42].

$$\rho_{nf} = (1 - \varphi)\rho_{nf} + \varphi\rho_s \quad (26)$$

$$(\rho C_p)_{nf} = (1 - \varphi)(\rho C_p)_f + \varphi(\rho C_p)_s \quad (27)$$

$$(\rho\beta)_{nf} = (1 - \varphi)\rho\beta_f + \varphi(\rho\beta)_s \quad (28)$$

$$\mu_{static} = \frac{\mu_f}{(1-\varphi)^{2.5}} \quad (29)$$

$$\alpha_{nf} = \frac{k_{nf}}{(\rho C_p)_{nf}} \quad (30)$$

For the present study both the static and Brownian thermal conductivity of the transport fluid particles are included in order to inspect the heat transfer performance of the nanofluids on the micropump where as k_{eff} is introduced to the model input for ultimate purpose.

$$k_{static} = \frac{k_s + 2k_f - 2\varphi(k_f - k_s)}{k_s + 2k_f\varphi(k_f - k_s)} k_f \quad (31)$$

$$k_{Brownian} = \frac{\varphi\rho_p C_{p,p}}{2} \sqrt{\frac{2K_B T_{ref}}{3\pi d \mu_{static}}} \quad (32)$$

$$k_{eff} = k_{static} + k_{Brownian} \quad (33)$$

In a similar manner to thermal conductivity, effective viscosity of the nanofluids are also looked out.

$$\mu_{eff} = \frac{\mu_f}{(1-\varphi)^{2.5}} + \frac{k_{Brownian}}{k_f} \times \frac{\mu_f}{Pr_f} \quad (34)$$

Mesh generation and convergency test

The total magneto hydrodynamic (MHD) micro pump system has been separated out into four subsystem – 1. Magnet domain, 2. Electrical domain, 3. Plastic domain (for pump construction purpose), 4. Fluid domain. In order to smooth the computational process of the MHD system all these subsystems except the acrylic plastic domain are discretized into free tetrahedral and triangular element. **Fig. 4** represents different views of the MHD micro pump with all of its distinct meshed parts. Close observation opens up the case that – coarse mesh is applied for the magnetic portion of the pump whereas fine mesh is implemented for the thin electrical Cu wire. A finer mesh has applied for the fluid region to study the heat transfer, velocity, pressure and temperature insight of the medium.

A grid independence test is conducted to understand when the applied numerical process achieved convergency. The convergency test is mainly carried out to reduce the computational load of the commercially available software and the computational time as well. **Fig. 5** represents guided convergence test of the paper for constant values of $Ri = 1$, $Ha = 5$, $Rd = 1$ and $\varphi = 0.05$ while two rudimentary parameters – average magnetic flux density (B_{avg}) and average electrical current intensity (I_{avg}) are chosen to illustrate insights of the test. It is to be found from the paper that the ultimate grid independence of the numerical procedure is achieved for element number around 21000. Trend lines of both the parameters show steady increase with the element number while the average magnetic flux intensity exhibits a more protean pattern compared to the magnitudes of average electrical current intensity.

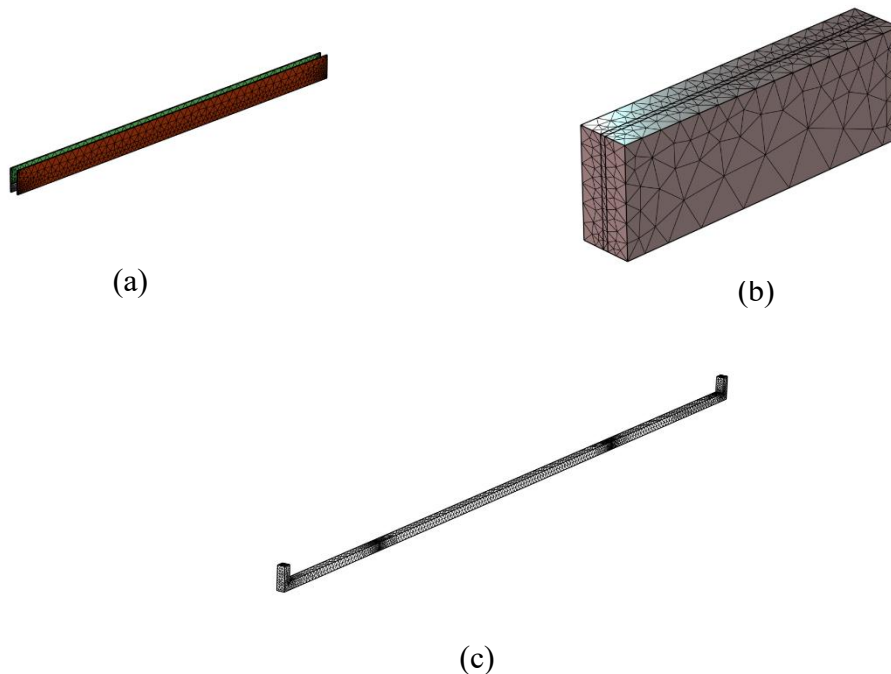


Fig. 4 Different views of discretized mesh parts of the proposed MHD pump – (a) Cu electrodes, (b) Neodymium magnet, (c) fluid domain.

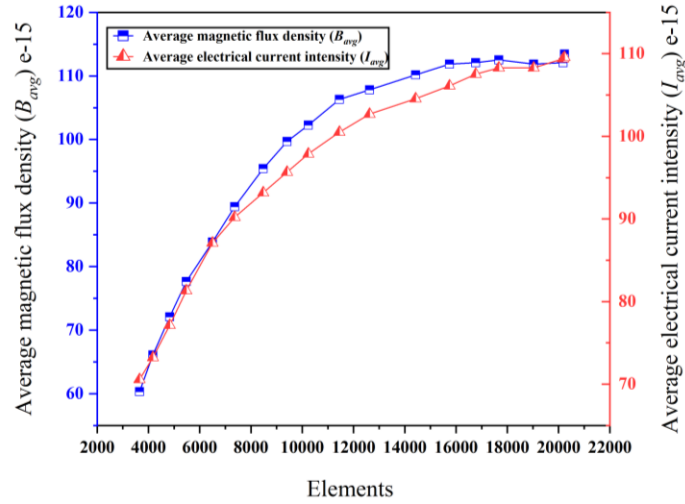


Fig. 5 Grid convergency test for the represented value at $Ri = 1$, $Ha = 5$, $Rd=1$ and $\varphi = 0.05$

Validation

Accuracy of the present study is analyzed against two different sets of numerical values obtained from Kosuke Ito et al. [43]. **Fig. 6** holds the relationship between electrical current, I and volume flow rate of transport liquid, Q under a constant magnetic flux density of 0.32T. The graph shows the difference in trends of the flow rate for present paper against both the experimental and numerical values of Kosuke et al [43]. A negligible amount of divergence can be seen for the proposed work when compared with validated paper at the initial small values of electrical current (~ 10 mA) however, the discordance is noticeable when the current value surpassed 15 mA or more. One core reason could be the formation of bubbles due to which velocity of the fluid flow decreases in the experimental set up of the project. However, the simulation might just ignore the bubbles formation for which the velocity of fluid flow maintains higher magnitude for numerical analysis of both papers while good proximity in outcomes can be observed within them.

Fig. 7 illustrates the change in maximum temperature against electric current for constant magnetic flux density of 0.5T. The outcome showed in the graph is for the MHD pump system devoid of any external uniform heat source and heat sink. Numerical analysis for both the paper shares sheer contiguity in term of generation of maximum temperature with respect to a continuously but steadily raising current. Looking at this plot along with the previous one it can be deduced that the present work is in nice accord with the one that has been pursued in Kosuke et al. [43] and therefore the computational procedure followed in current study is retained to advance further. All the necessary numerical conditions applied for the validation of the work is tabulated in **Table 1**.

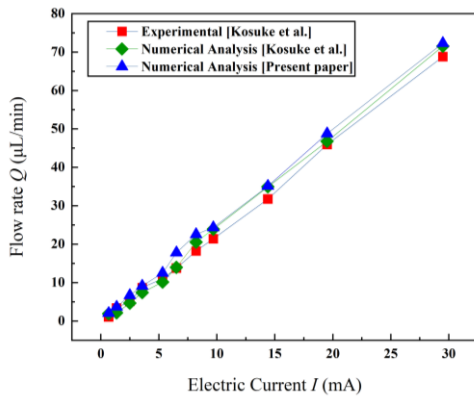


Fig. 6 Comparison of the flow rate Q between present paper and Kosuke et al [43].

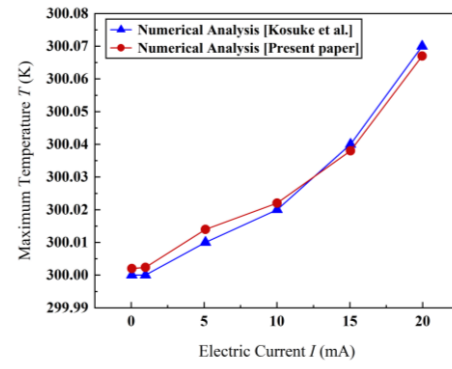


Fig. 7 Comparison of the maximum temperature between present paper and Kosuke et al [43].

Table 1

Working fluid	PBS (Phosphate buffered saline)
Magnetic flux density B_z	0.32T – 0.5T
Initial temperature T_o	300 K
Applied electric current I	0 mA – 30 mA
Time step ∂t	5×10^{-6} s

Result and discussion

This corresponding section presents the radiation effect of three different blood-based hybrid nanofluids – Ag, Cu₂O and Ti₂O upon fluid, magnetic and electrical properties of the MHD micropump. To present outcomes of the study velocity distribution, pressure drop and temperature gradient along the flow path of the micropump for different nanofluids are numerically investigated under the scope of two dimensionless parameters – Rd and Re . *Radiation number (Rd)* is the parameter that denotes the emitted thermal radiation from the radioactive fluids which are used as transport medium in the study whereas *Reynold's number (Re)* signifies the forced convective heat transfer due to the bulk motion of the hybrid bio-convective nanofluids. Focusing on these two parameters, two other fundamental properties of the MHD micropump – MFD (*magnetic flux density*) and EFI (*electric flux intensity*) along with fluid properties are tabulated in three distinct kinds of visualization techniques. Line and surface plots are referred for visualizing the results for one-to-one correspondence of the data as well as their distribution along the pump surface. Volume plots (3D plots) are also conferred here in this study to provide the readers a more meaningful insight about how the properties behave when blood based radioactive bio-convective nanofluids are used as the transport medium in human body for advanced biomedical applications. Also, line plots infers comparative performance analysis of the selected blood based nanofluids with respect to mentioned MHD parameters while the surface and volume plots confer interdependence between forced convective heat transfer and radiative heat transfer of the nanofluids upon the same parameters.

6.1. Effect of radiation on average velocity distribution along flow channel of the MHD micropump

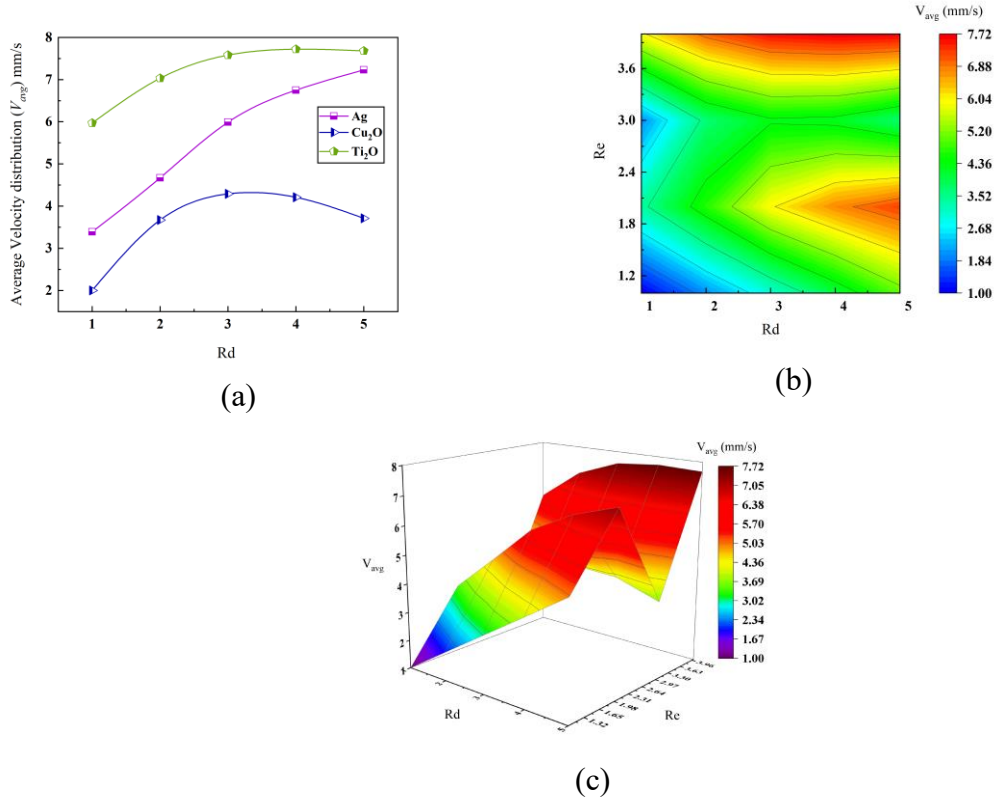


Fig. 8 Effect of Radiation number Rd and Reynold's number Re on velocity distribution.

Fig. 8 depicts the line plot, surface plot and volume plot of velocity distribution through MHD micro channel of the pump when considering both the radiative and convective heat transfer. **Fig. 8 (a)** illustrates impact of radiation parameter on average velocity distribution, V_{avg} for three different blood-based nanoparticles – Ag, Cu_2O and Ti_2O . From the line plot it can be seen that maximum average velocity is observed for Ag and Ti_2O under the maximum radiation number of 5. For Cu_2O maximum velocity of 4 mm/s is obtained when $Rd = 3$. Although all three of the lines show positive quadratic correlations between the average velocity and radiation parameter, their behavioral curves are different from one another. Ti_2O and Ag exhibits steady progress in their velocity magnitude with respect to Rd as Ti_2O saturates with its maximum value of 7.77 mm/s for $Rd = 3$ to $Rd = 5$ while Ag provides a steep increment to a value of 7 mm/s for the same range. Cu_2O starts to exhaust its average velocity magnitude from $Rd = 3$ to $Rd = 5$ after reaching its peak value which showcases debility of Cu_2O in transporting fluid medium under heavy radiation source when used along with blood for any intravenous treatment. The other two nanofluids – Ag and Ti_2O show decent transportation feasibility while Ti_2O being came out as the steadier one between the two under a range of radiation values.

An understandable relationship between forced convective bulk flow and thermal radiation over velocity distribution for the micro channel of MHD micropump has been exhibited in **Fig. 8 (b)**

and Fig. 8 (c). The former contour graph features a range of Reynold's number that are obtained for velocity distribution through the channel and Rd values ranging from 0 to 5. It is to be noted from the plot maximum velocity is obtained for maximum Rd value of 5 and maximum Re value of 3.6 which implies that velocity through micro channel is largely dominated by both forced convection and thermal radiation. However, moderate nanofluid flow can be seen for $Re = 2.4$ to $Re = 3.6$ even when $Rd = 5$ and so it can be anticipated that the fluid flow is mostly influenced by the forced convection phenomena. Alternatingly a contradiction to this anticipation is found when nearly maximum magnitude of velocity is observed for $Re = 1.8$ to $Re = 2.4$ while Rd remaining at its highest value. Similarly, lean velocity profiles are noticed for low to moderate values of Rd ($Rd = 1$ to $Rd = 3$) even when forced convection is highest and the velocity distribution gets stronger as the Rd value increases. Considering both of these observation, it can be deduced that average velocity distribution through the microchannel is largely controlled by the radiation number and thereby more susceptible to radiative behavior of the nanofluids that are used in blood flow compared to the forced bulk flow of those. Fig.1 (c) provides a more robust demonstration of the interdependence among forced bulk flow (Re) and radiative nature (Rd) and average velocity distribution (V_{avg}) for the applied nanofluids in this study.

6.2. Effect of radiation on average pressure drop along flow channel of the MHD micropump

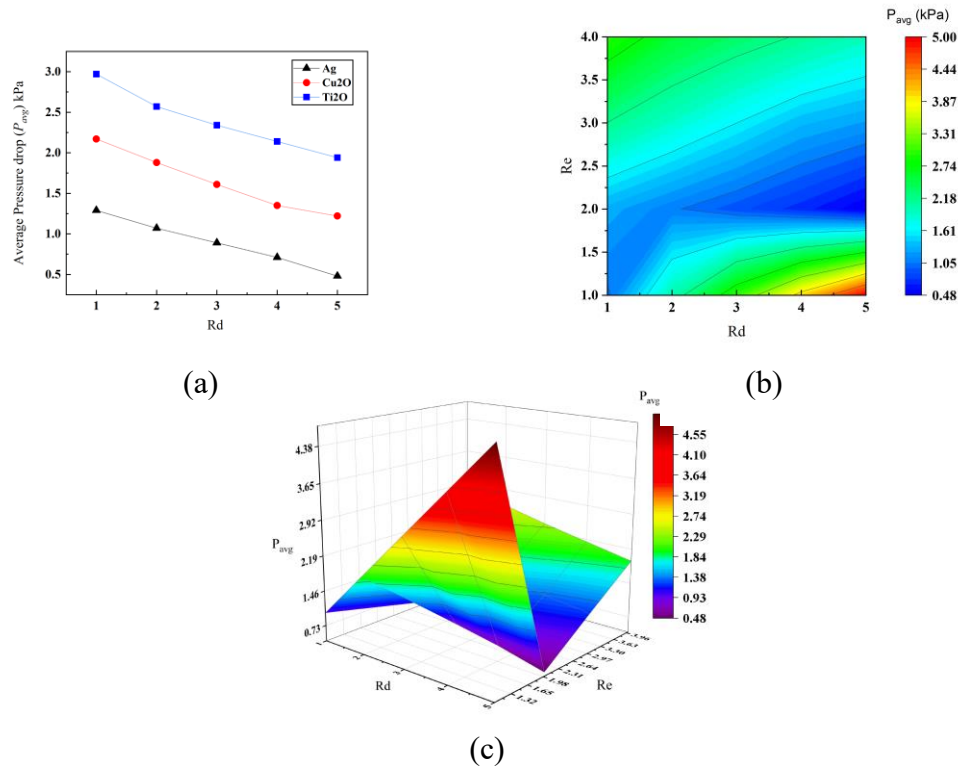


Fig. 9 Effect of Radiation number Rd and Reynold's number on pressure drop across the flow channel.

The functional pivot of MHD micropump system is generation of sufficient pressure drop by Lorentz force so that transporting medium can flow through narrow and shallow paths. Such

pressure drop characteristics of a MHD micropump is of great interest as it dictates how efficiently the micropump will operate under conditioning circumstances. This characteristic for the proposed MHD micropump has been illuminated in terms of forced convection and radiative heat transfer for three different blood based nanofluids – Ag, Cu₂O and Ti₂O in **Fig. 9**. A comparative performance in pressure drop for the mentioned nanofluids is presented in **Fig. 9** (a) which avails a liner regressive relationship between pressure loss through the pump microchannel and its radiative parameter. For all the three nanofluids maximum pressure is observed for $R_d = 1$ whereas minimum value for $R_d = 5$. For minimum value of R_d , Ti₂O is found to be the most expediting nanofluid among the three whereas Ag is the least however, while considering radiative impact on the same nanofluids – Ti₂O suffered relative pressure drop of 25% (3 kPa to 2.25 kPa) while Ag has the most with 60% (1.25 kPa to 0.5 kPa). Cu₂O follows a mediatory value in between the earlier nanofluids with a relative manner of 22% (2.25 kPa to 1.5 kPa). Larger pressure drop across the microchannel will nothing but only increase proportionate pumping power of the MHD micropump which in turns will require higher magnitude of Lorentz force. This will correspond to elevated demand of electromagnetic force which is fairly intricate to generate in a MHD pump of micro scale. Evaluating the performance of the selected nanofluids under this circumstance, Cu₂O and Ti₂O are proved to be the most equipped nanoparticles in blood transportation for their relatively less pressure loss while Ag renders maximum of its kind.

Fig. 9 (b) corresponds interdependency of forced convection (Re) and radiative flux (R_d) on the average pressure drop through microchannel of MHD pump. From the contour plot it is found that maximum pressure drop occurs for maximum value of R_d and minimum value of Re ($R_d = 5$ and Re ranging from $Re = 1$ to $Re = 1.25$). However, when Re value increases from $Re = 1.25$ to $Re = 4$ and R_d remains constant at $R_d = 5$, average pressure drop seems to get dropped significantly. Similar phenomena can be seen when pressure loss becomes moderate to negligible for increasing value of Re ($Re = 1$ to $Re = 3$) even when there is sufficient rise in R_d value ($R_d = 1$ to $R_d = 4$). Reflecting over the interaction between these two non-dimensional parameters it can be stated that – at lesser radiative environment the pressure drop is mostly dominated by radiation flux whereas at higher radiation value it is dictated by forced convective bulk motion of transporting medium. A good insight out of this observation is to use nanofluids with moderate radiation nature while maintaining a decent in channel flow through the pump for proper intravenous sedation treatment. **Fig. 9** (c) dedicates the interaction among the three parameters in a more rigorous manner. Maximum pressure drop occurs (~2.95 kPa to 4.89 kPa) for $R_d = 4$ to $R_d = 5$ while the flow seeping through the channel with $Re = 1.01$ to $Re = 1.98$ as can be seen from the three-dimensional volume plot.

6.3. Effect of radiation on average temperature gradient along flow channel of the MHD micropump

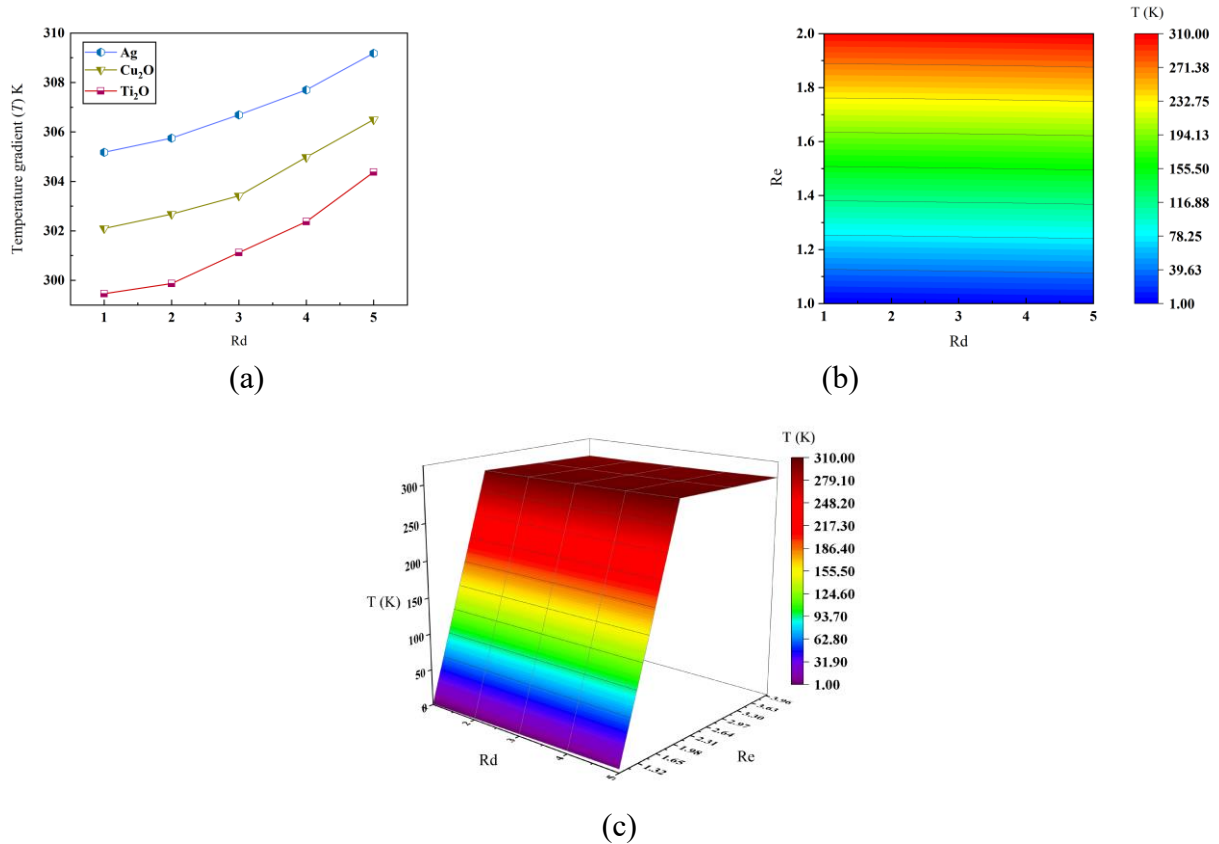


Fig. 10 Effect of Radiation number Rd and Reynold's number Re on temperature gradient along the flow channel.

Investigation of average temperature drop along the flow channel of MHD micropump is of great importance. Higher pumping of fluid through the microchannel increases pressure drop which in turn increases temperature non-uniformity along the flow path. Temperature gradient of higher magnitude will make the MHD micropump hotter during operation and radiates heat. This will make the pump quite vulnerable to system failure. **Fig. 10** (a) represents temperature gradient of the proposed blood based nanofluids during their bulk motion along the channel. It illuminates that maximum temperature has been observed for Ag while minimum is seen for Ti_2O with value of 309 K and 303 K respectively. However, temperature gradient is found to be least for Cu_2O with a relative value of 0.98% while both Ti_2O and Ag transcendent value of 1.65% and 1.29% respectively. A relatively moderate maximum temperature with the least temperature gradient makes Cu_2O the desired bioconvective nanofluid among the selected threes. However initial temperature rise during injection of the fluid is much less for Ti_2O , moderate for Cu_2O and higher for Ag. Initiating temperature (temperature during injection) reflects the temperature variation within human body which signifies the suitability of amalgamation of nanofluid with human blood as a moderate to optimal temperature is required for proper combination of any nanoparticles with human blood – an important prospect to consider Cu_2O as the transportation medium coolant.

The contour surface plot presented in **Fig. 10** (b) manifests variation of forced convective flow with respect to radiation parameter and average temperature gradient. It is to be found that the average temperature gradient is sharply regulated by Re number rather than Rd values as higher Re value (Re = 1.8 to Re = 2) corresponds to maximum temperature drop of 309~310 K. The outcome seems to be remained same even though Rd values rises from Rd = 1 to Rd = 5. The temperature gradient drops considerably for lower Re values however maintains a relatively stable temperature dissipation (116 K~238 K) for Re = 1.4 to Re = 1.8. Since the results show that temperature gradient through the channel is mostly dominated by Re number, it can be declared that a moderate forced convective bulk flow of the nanofluids should be considered through the pump for smooth dispersion of heat as it is much sensitive towards forced convection and any contemplation regarding radiative flux can be ignored for this purpose. **Fig. 10** (c) provides a more insightful and details knowledge of how temperature gradient being a strong function of Re number as can be seen and it is also noted that the relationship among all the three parameters follows a positive linear relationship.

6.4. Effect of radiation on average magnetic flux density along flow channel of the MHD micropump

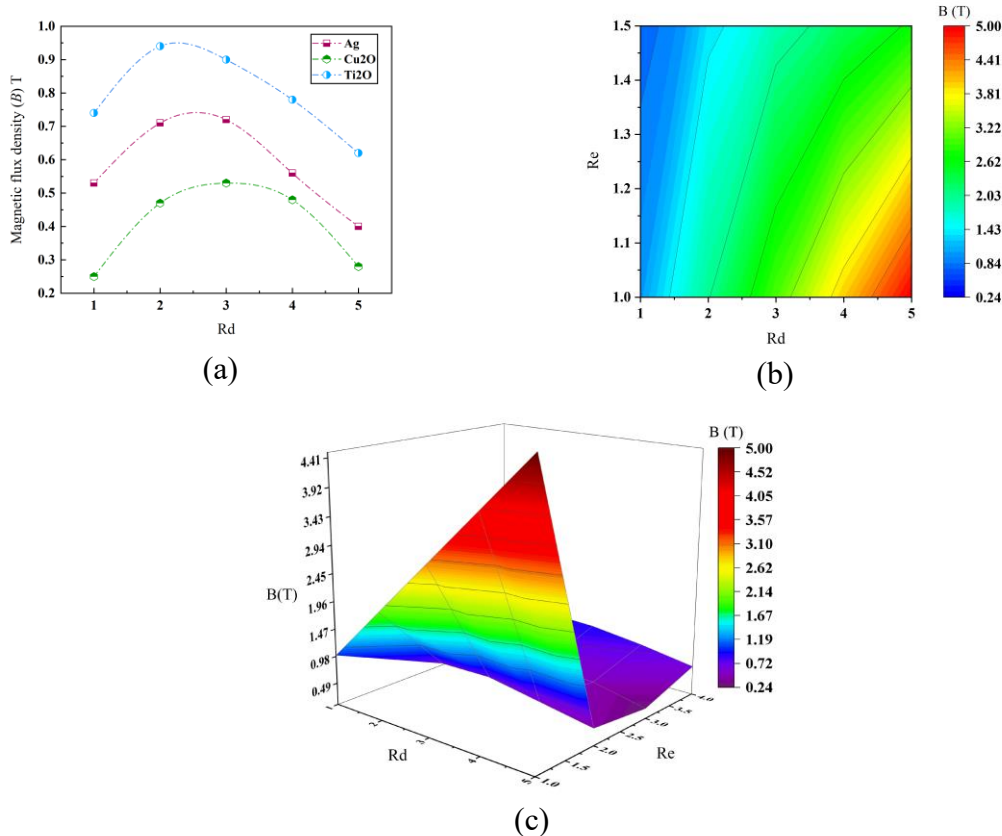


Fig. 11 Effect of Radiaton number Rd and Reynold's number Re on average magnetic flux density.

Magnetic flux density (B) of a MHD micropump denotes the magnetic behavior of the pump when Magnetic nanofluids are used along with blood as transport medium. **Fig. 11** (a) showcases such performance of the established pump for three different nanofluids. From the graph it is to be noted that up to a certain range of Rd number magnetic flux density (B) of all three nanofluids rises. For a very specific value of Rd magnetic flux reaches a maximal point and then decreases with the reduction in radiation flux although that inflection point is different for different nanofluids. The magnetic flux density characteristic curves for all the nanofluids approximate “bell curve” or “a normal distribution curve”. Maximum magnetic flux density is achieved for Ti_2O with a value of 0.95T while Ag and Cu_2O follows it with values of 0.712T and 0.5T respectively. Higher magnetic flux density implies added strength of the generated magnetic field within a channel for any particles, in this case – the nanofluids used for transporting blood. Richer magnetic flux density corresponds to stronger electromagnetic flux and thereby providing more enriched Lorentz force which is the source of operation of MHD micropump. For the present paper – Ti_2O is supposed to be the equipped nanofluid to provide sufficient magnetic flux density out of the three nanofluids for proper operation of the nanofluids. One of the good reasons behind this might be the dipolar moment within the Ti_2O atoms and when combined with the externally applied static magnetic flux – it amplifies the electromagnetic force of the domain. The other nanoparticles – Cu_2O and Ag bestow relatively lower magnetic flux density however magnetic flux loss is the least for Cu_2O which results in a more stable electromagnetic force.

Fig. 11 (b) represents surface plot of the microchannel which describes the interrelatedness among two dimensionless parameters – Rd and Re with average magnetic flux density. The illustration confers variation of forced convection (Re) and radiation behavior (Rd) with respect to each other and magnetic flux as well. Magnetic flux density of highest magnitude is obtained for maximum Rd value of $Rd = 5$ while Re ranges from $Re = 1$ to $Re = 1.2$. Contrarily, least to moderate level of magnetic flux is showed up for $Re = 1.25$ to $Re = 1.5$ for $Rd = 1$ to $Rd = 4$. An interesting point is to be spot that average magnetic flux density is mostly governed by radiation parameter and relatively less by forced convective flow the nanofluid. This simple phenomena can be carried out to understand the fact that nanofluid comprised blood flow through MHD microchannel might engender stronger magnetic flux and thereby stronger electromagnetic field if their magnitude of self-radiation is higher; however, the related compensation to human body is to be sincerely acknowledged. **Fig. 11** (c) corresponds to a more insightful exposition of the abovementioned discussion and showpieces a three-dimensional contour plot to visualize it. It refers to maximum B with a value of 2.94T which is obtained for around $Re = 1$ and $Rd = 4$ to $Rd = 5$.

6.5. Effect of radiation on average electric flux intensity along flow channel of the MHD micropump

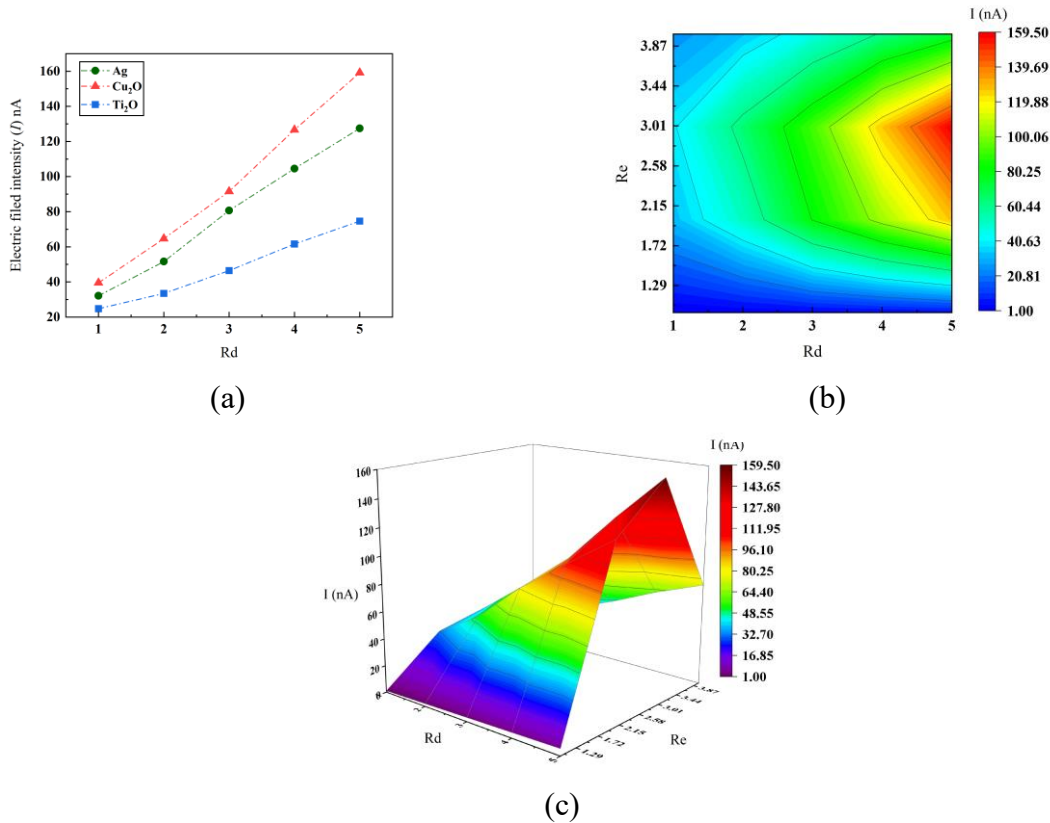


Fig. 12 Effect of Radiation number Rd and Reynold's number Re on average electric flux intensity.

Fig. 12 (a), (b) and (c) demonstrates the line plot, contour surface plot and contour volume plot of average electric flux intensity of the MHD pump's microchannel for three different plasma based nanofluids. **Fig. 12** (a) illustrates the comparative performance of the selected nanofluids with respect to Rd values – Cu_2O and Ag are among the highest generators of electric flux intensity with proximate values of 160 nA and 123 nA. Ti_2O provides relatively lesser electric flux with a magnitude of 67 nA. However, while comparing the intensity drop of the electric field it can be found that the flux density drop is maximum for Cu_2O and Ag follows it to the second with a value of 75% and 72.59% respectively. Ti_2O is the least considering drop of electric density with a value of 60.33%. Lesser electric flux density droppage refers to more stable generation of electric force and thereby more consistent generation of electromagnetic force. Effective electromagnetic force will help the pump to overcome frictional and mechanical losses within the system and increases its efficiency. However, operating at higher radiative environment it is more important to provide sufficient electric flux even though a rapid change is seen in flux density for the nanofluid as it requires higher flow of electromagnetic force which in return demands higher magnitude of electric flux. Considering this – Cu_2O is supposed to be the most preferred nanofluid among all the three due to its highest level of electric flux generation for $Rd = 5$.

The surface plot in **Fig. 12** (b) reveals the contour plot of the microchannel as a functions of two different dimensionless parameters – Re and Rd with average electric flux intensity (I). Maximum electric flux is observed for Rd = 4 to Rd= 5 while the forced convective flow Re is in between Re = 1.90 to Re = 3.24. On the other hand, electric flux becomes much lower at higher Rd value but less Re value (Rd = 2 to Rd = 5, Re = 1 to Re = 1.72) which dictates that the average electric flux intensity is independent of the radiative flux at lesser forced convection that is to say the lesser electric force is achieved whenever the forced bulk motion of nanofluids is relatively low. The concept is even true for higher Re values also (Rd = 2 to Rd = 5, Re = 3.20 to Re - 3.87) however the electric flux becomes moderate at this range. Following the overall scenario, it can be said that the microchannel pursues richer electric field intensity in a relative manner to the radiative nature of the flow which is higher for higher radiative nanofluids and less governed by certain changes in Re. **Fig. 12** (c) repeats the same incident however with more focused details – obtaining highest level of I_{avg} (nA) at nearly 160 nA while Rd ranges from Rd = 4 to Rd = 5 and Re = 2.15 to Re = 3.87.

Conclusion

The study carried out focuses on the radiative behavior of different blood based biological nanofluids – Ti₂O, Ag and Cu₂O when used in MHD micropump. Qualitative analysis for the proposed subject has been performed in terms of fluidic properties – temperature gradient, velocity distribution, pressure drop, magnetic property – magnetic flux density and electrical property – electrical flux intensity. The ultimate outcomes from the study can be outlined into the followings –

1. Velocity distribution analysis provides Ti₂O as the most efficient radiative biomedical nanoparticles when used with blood stream. Average velocity distribution along the micropump channel is dominated by the radiation characteristics of the nanoparticles rather than its forced bulk motion.
2. Cu₂O and Ti₂O are found to be the nanoparticles generating least pressure drop while operating in high radiative surrounding in MHD pump. The pressure drop plots recognize a moderate combination of radiation flux with forced convection is fine for a smooth and efficient blood flow during microscale IV treatment.
3. From the study particularly focusing on average temperature gradient, it is found that Cu₂O is the one with lest temperature gradient for a range radiation values which makes it a relatively stable nanofluid to unify with blood. Temperature characteristics contours reveal that temperature gradient in the presence of radiative environment is strongly governed by the forced convection of nanofluid amalgamed blood flow over their radiation strength.
4. Magnetic flux density curve showcases that Ti₂O instigates maximum magnetic flux density among the three other nanofluids and assists in generation of higher electromagnetic force in pumping blood as IV fluids in maintaining hydration, fluid balance and necessary nutrients. However, the contour surface plots of same study also conforms with higher magnetic flux density necessitates higher radiation generation which is a concern for general IV treatment.

5. Cu_2O is the most desired nanofluid as per the exploration of electric flux intensity due to its expediting electrical nature under radiation circumstances as it follows observable attribute with respect to changes in radiation values - which is to be negotiated sincerely while providing low radiative therapy.

Considering the computational excerpts provided – Ti_2O is thought to be the most effective nanofluid for blood based intravenous treatments such as – IV chemotherapy, IV coagulants, IV pain medications etc. due to its superiority over other nanoparticles in terms of the properties defined earlier.

Conflict of interest

It is to be declared that as per the knowledge of all the authors there is no active or passive financial and personal interest that could have impacted the work as well as the outcome reported in the paper.

Appendix/Nomenclature

<i>MHD</i>	Magneto Hydrodynamic
<i>BL</i>	Blood
<i>Cu₂O</i>	Copper oxide
<i>Ag</i>	Silver
<i>Ti₂O</i>	Titanium oxide
<i>MFD</i>	Magnetic field density
<i>EFI</i>	Electric field intensity.
<i>Rd</i>	Radiation parameter
<i>Re</i>	Reynolds number
<i>Al</i>	Aluminum
<i>x, y, z</i>	Dimensional cartesian coordinates
ρ	Density
<i>D</i>	Electric displacement field
<i>B</i>	Magnetic field
<i>E</i>	Electric field
<i>H</i>	Magnetic field intensity
<i>J</i>	Electric current density
<i>t</i>	Time
∇	Vector differential operator
<i>u, v</i>	Velocity components
<i>nf</i>	Nanofluid
μ	Dynamic viscosity
<i>P</i>	Pressure
<i>T</i>	Temperature
α	Thermal diffusivity
ϑ	Kinematic viscosity
<i>q</i>	External heat flux

C_p	Reynolds number
C	Cold system
K	Thermal conductivity
φ	Non dimensional temperature
V	Applied electrical voltage
L	Length of pump
U, V	Dimensionless velocity components
N	Any direction
X, Y	Dimensionless cartesian coordinates
avg	Average value
β	Thermal expansion coefficient
s	Solid
f	Fluid
Pr	Prandtl number
I	Electric current
η	Dimensional optical thickness
σ	Electrical conductivity
in	Inlet
out	Outlet
IV	Intravenous

References

- [1] P. A. Davidson and E. V. Belova, "An Introduction to Magnetohydrodynamics," *Am. J. Phys.*, vol. 70, no. 7, pp. 781–781, 2002, doi: 10.1119/1.1482065.
- [2] P. A. Davidson, "Magnetohydrodynamics in materials processing," *Annu. Rev. Fluid Mech.*, vol. 31, pp. 273–300, 1999, doi: 10.1146/annurev.fluid.31.1.273.
- [3] A. Shahidian, M. Ghassemi, S. Khorasanizade, M. Abdollahzade, and G. Ahmadi, "Flow analysis of non-Newtonian blood in a magnetohydrodynamic pump," *IEEE Trans. Magn.*, vol. 45, no. 6, pp. 2667–2670, 2009, doi: 10.1109/TMAG.2009.2018954.
- [4] D. Chatterjee and S. Amiroudine, "Lattice Boltzmann simulation of thermofluidic transport phenomena in a DC magnetohydrodynamic (MHD) micropump," *Biomed. Microdevices*, vol. 13, no. 1, pp. 147–157, Feb. 2011, doi: 10.1007/S10544-010-9480-8/TABLES/2.
- [5] A. Shahidian and M. Ghassemi, "Effect of magnetic flux density and other properties on temperature and velocity distribution in magnetohydrodynamic (MHD) pump," *IEEE Trans. Magn.*, vol. 45, no. 1, pp. 298–301, 2009, doi: 10.1109/TMAG.2008.2008614.
- [6] A. J. Chamkha, S. K. Jena, and S. K. Mahapatra, "MHD Convection of Nanofluids: A Review," *J. Nanofluids*, vol. 4, no. 3, pp. 271–292, 2015, doi: 10.1166/jon.2015.1166.
- [7] V. D. Dhareppagol, A. Saurav, and V. P. P. G. Halakatti, "The Future Power Generation with MHD Generators Magneto Hydro Dynamic generation ...," *Int. J. Adv. Electr. Electron. Eng.*, pp. 101–105, 2013.

- [8] A. Abid and M. T. Sarowar, "Heat Transfer, Thermal Stress and Failure Inspection of a Gas Turbine Compressor Stator Blade Made of Five Different Conventional Superalloys and Ultra-High-Temperature Ceramic Material: A Direct Numerical Investigation," *J. Fail. Anal. Prev.*, vol. 22, no. 3, pp. 878–898, Jun. 2022, doi: 10.1007/S11668-022-01413-W/FIGURES/9.
- [9] A. K. Azad, A. Abid, C. N. Mithun, M. J. Hasan, R. Hossain, and M. M. Rahman, "Effect of Richardson number on transient double diffusive mixed convection: A thermohydrodynamic study," *Int. J. Thermofluids*, vol. 17, p. 100273, Feb. 2023, doi: 10.1016/J.IJFT.2022.100273.
- [10] A. Abid and A. A. Bhuiyan, "A finite element analysis approach to design and optimize the static structural impact on a skateboard," *Mater. Today Proc.*, vol. 60, pp. 2171–2187, Jan. 2022, doi: 10.1016/J.MATPR.2022.02.424.
- [11] M. I. Hasan, A. J. F. Ali, and R. S. Tufah, "Numerical study of the effect of channel geometry on the performance of Magnetohydrodynamic micro pump," *Eng. Sci. Technol. an Int. J.*, vol. 20, no. 3, pp. 982–989, Jun. 2017, doi: 10.1016/J.JESTCH.2017.01.008.
- [12] M. E. Moghadam and M. B. Shafii, "Rotary magnetohydrodynamic micropump based on slug trapping valve," *J. Microelectromechanical Syst.*, vol. 20, no. 1, pp. 260–269, Feb. 2011, doi: 10.1109/JMEMS.2010.2090500.
- [13] J. Azimi, M. Zakeri, and M. Javidfard, "A numerical study on characteristics of the magnetohydrodynamic micropumps," *Int. Conf. Robot. Mechatronics, ICROM 2015*, pp. 401–405, Dec. 2015, doi: 10.1109/ICROM.2015.7367818.
- [14] S. Lim and B. Choi, "A study on the MHD (magnetohydrodynamic) micropump with side-walled electrodes," *J. Mech. Sci. Technol.*, vol. 23, no. 3, pp. 739–749, Jun. 2009, doi: 10.1007/S12206-008-1107-0/METRICS.
- [15] H. Duwairi and M. Abdullah, "Thermal and flow analysis of a magneto-hydrodynamic micropump," *Microsyst. Technol.*, vol. 13, no. 1, pp. 33–39, Jan. 2007, doi: 10.1007/S00542-006-0258-0/FIGURES/9.
- [16] E. E. Tzirtzilakis, "A mathematical model for blood flow in magnetic field," vol. 077103, 2005, doi: 10.1063/1.1978807.
- [17] M. M. Bhatti and M. Ali Abbas, "Simultaneous effects of slip and MHD on peristaltic blood flow of Jeffrey fluid model through a porous medium," *Alexandria Eng. J.*, vol. 55, no. 2, pp. 1017–1023, 2016, doi: 10.1016/j.aej.2016.03.002.
- [18] P. J. Wang, C. Y. Chang, and M. L. Chang, "Simulation of two-dimensional fully developed laminar flow for a magneto-hydrodynamic (MHD) pump," *Biosens. Bioelectron.*, vol. 20, no. 1, pp. 115–121, Jul. 2004, doi: 10.1016/J.BIOS.2003.10.018.
- [19] Asifa, T. Anwar, P. Kumam, Z. Shah, and K. Sithithakerngkiet, "Significance of Shape Factor in Heat Transfer Performance of Molybdenum-Disulfide Nanofluid in Multiple Flow Situations; A Comparative Fractional Study," *Mol. 2021, Vol. 26, Page 3711*, vol. 26, no. 12, p. 3711, Jun. 2021, doi: 10.3390/MOLECULES26123711.
- [20] K. Ramesh and J. Prakash, "Correction to: Thermal analysis for heat transfer enhancement


- in electroosmosis-modulated peristaltic transport of Sutterby nanofluids in a microfluidic vessel (Journal of Thermal Analysis and Calorimetry, (2019), 138, 2, (1311-1326), 10.1007/s10973-018-7939-7),” *J. Therm. Anal. Calorim.*, vol. 138, no. 2, pp. 1327–1328, Oct. 2019, doi: 10.1007/S10973-019-08148-1/FIGURES/1.
- [21] A. Zaib, U. Khan, A. Wakif, and M. Zaydan, “Numerical Entropic Analysis of Mixed MHD Convective Flows from a Non-Isothermal Vertical Flat Plate for Radiative Tangent Hyperbolic Blood Biofluids Conveying Magnetite Ferroparticles: Dual Similarity Solutions,” *Arab. J. Sci. Eng.*, vol. 45, no. 7, pp. 5311–5330, Jul. 2020, doi: 10.1007/S13369-020-04393-X/FIGURES/24.
- [22] W. Alghamdi, A. Alsubie, P. Kumam, A. Saeed, and T. Gul, “MHD hybrid nanofluid flow comprising the medication through a blood artery,” *Sci. Reports 2021 111*, vol. 11, no. 1, pp. 1–13, Jun. 2021, doi: 10.1038/s41598-021-91183-6.
- [23] S. Venkateswarlu, S. V. K. Varma, and R. V. M. S. S. Kiran Kumar, “Thermo-diffusion and non-uniform heat source/sink effects on hydromagnetic flow of Cu and TiO₂ water - based nanofluid partially filled with a porous medium,” *Informatics Med. Unlocked*, vol. 13, pp. 51–61, Jan. 2018, doi: 10.1016/J.IMU.2018.10.005.
- [24] N. Mahato, S. M. Banerjee, R. N. Jana, and S. Das, “MoS₂-SiO₂/EG hybrid nanofluid transport in a rotating channel under the influence of a strong magnetic dipole (Hall effect),” *Multidiscip. Model. Mater. Struct.*, vol. 16, no. 6, pp. 1595–1616, Oct. 2020, doi: 10.1108/MMMS-12-2019-0232/FULL/PDF.
- [25] J. Prakash, A. Sharma, and D. Tripathi, “Thermal radiation effects on electroosmosis modulated peristaltic transport of ionic nanoliquids in biomicrofluidics channel,” *J. Mol. Liq.*, vol. 249, pp. 843–855, Jan. 2018, doi: 10.1016/J.MOLLIQ.2017.11.064.
- [26] B. Mallick, J. C. Misra, and A. R. Chowdhury, “Influence of Hall current and Joule heating on entropy generation during electrokinetically induced thermoradiative transport of nanofluids in a porous microchannel,” *Appl. Math. Mech. 2019 4010*, vol. 40, no. 10, pp. 1509–1530, Oct. 2019, doi: 10.1007/S10483-019-2528-7.
- [27] M. Irfan, W. A. Khan, M. Khan, and M. Waqas, “Evaluation of Arrhenius activation energy and new mass flux condition in Carreau nanofluid: dual solutions,” *Appl. Nanosci.*, vol. 10, no. 12, pp. 5279–5289, Dec. 2020, doi: 10.1007/S13204-020-01449-0/METRICS.
- [28] M. K. Nayak, S. Shaw, and A. J. Chamkha, “3D MHD Free Convective Stretched Flow of a Radiative Nanofluid Inspired by Variable Magnetic Field,” *Arab. J. Sci. Eng.*, vol. 44, no. 2, pp. 1269–1282, Feb. 2019, doi: 10.1007/S13369-018-3473-Y/METRICS.
- [29] K. Jyothi, P. Sudarsana Reddy, and M. Suryanarayana Reddy, “Influence of magnetic field and thermal radiation on convective flow of SWCNTs-water and MWCNTs-water nanofluid between rotating stretchable disks with convective boundary conditions,” *Powder Technol.*, vol. 331, pp. 326–337, May 2018, doi: 10.1016/J.POWTEC.2018.03.020.
- [30] D. Pal, G. Mandal, and K. Vajravelu, “MHD convection–dissipation heat transfer over a non-linear stretching and shrinking sheets in nanofluids with thermal radiation,” *Int. J. Heat Mass Transf.*, vol. 65, pp. 481–490, Oct. 2013, doi: 10.1016/J.IJHEATMASSTRANSFER.2013.06.017.

- [31] A. Dawar, Z. Shah, P. Kumam, W. Khan, and S. Islam, "Influence of MHD on Thermal Behavior of Darcy-Forchheimer Nanofluid Thin Film Flow over a Nonlinear Stretching Disc," *Coatings 2019, Vol. 9, Page 446*, vol. 9, no. 7, p. 446, Jul. 2019, doi: 10.3390/COATINGS9070446.
- [32] P. Agrawal, P. K. Dadheech, R. N. Jat, D. Baleanu, and S. D. Purohit, "Radiative MHD hybrid-nanofluids flow over a permeable stretching surface with heat source/sink embedded in porous medium," *Int. J. Numer. Methods Heat Fluid Flow*, vol. 31, no. 8, pp. 2818–2840, Aug. 2021, doi: 10.1108/HFF-11-2020-0694/FULL/PDF.
- [33] S. S. Ghadikolaei, K. Hosseinzadeh, and D. D. Ganji, "Numerical study on magnetohydrodynamic CNTs-water nanofluids as a micropolar dusty fluid influenced by non-linear thermal radiation and joule heating effect," *Powder Technol.*, vol. 340, pp. 389–399, Dec. 2018, doi: 10.1016/J.POWTEC.2018.09.023.
- [34] S. Ahmed and H. Xu, "Forced convection with unsteady pulsating flow of a hybrid nanofluid in a microchannel in the presence of EDL, magnetic and thermal radiation effects," *Int. Commun. Heat Mass Transf.*, vol. 120, p. 105042, Jan. 2021, doi: 10.1016/J.ICHEATMASSTRANSFER.2020.105042.
- [35] P. B. A. Reddy, "Biomedical aspects of entropy generation on electromagnetohydrodynamic blood flow of hybrid nanofluid with nonlinear thermal radiation and non-uniform heat source/sink," *Eur. Phys. J. Plus*, vol. 135, no. 10, pp. 1–30, 2020, doi: 10.1140/epjp/s13360-020-00825-7.
- [36] I. Tlili, N. N. Hamadneh, W. A. Khan, and S. Atawneh, "Thermodynamic analysis of MHD Couette–Poiseuille flow of water-based nanofluids in a rotating channel with radiation and Hall effects," *J. Therm. Anal. Calorim.*, vol. 132, no. 3, pp. 1899–1912, Jun. 2018, doi: 10.1007/S10973-018-7066-5.
- [37] J. K. Patra *et al.*, "Nano based drug delivery systems: recent developments and future prospects," *J. Nanobiotechnology*, vol. 16, no. 1, p. 71, Sep. 2018, doi: 10.1186/S12951-018-0392-8.
- [38] P. Valipour and S. E. Ghasemi, "Numerical investigation of MHD water-based nanofluids flow in porous medium caused by shrinking permeable sheet," *J. Brazilian Soc. Mech. Sci. Eng.*, vol. 38, no. 3, pp. 859–868, Mar. 2016, doi: 10.1007/S40430-014-0303-3/FIGURES/11.
- [39] E. Haile and B. Shankar, "A Steady MHD Boundary-Layer Flow of Water-Based Nanofluids over a Moving Permeable Flat Plate," *Int. J. Math. Res.*, vol. 4, no. 1, pp. 27–41, 2015, doi: 10.18488/JOURNAL.24/2015.4.1/24.1.27.41.
- [40] M. Veera Krishna, N. Ameer Ahamad, and A. J. Chamkha, "Radiation absorption on MHD convective flow of nanofluids through vertically travelling absorbent plate," *Ain Shams Eng. J.*, vol. 12, no. 3, pp. 3043–3056, Sep. 2021, doi: 10.1016/J.ASEJ.2020.10.028.
- [41] S. Dinarvand and A. J. Chamkha, "Blood-based hybrid nano fluid flow through converging / diverging channel with multiple slips effect : a development of Jeffery-Hamel problem," 2022, doi: 10.1108/HFF-08-2022-0489.


- [42] M. Awais, M. Saad, H. Ayaz, M. M. Ehsan, and A. A. Bhuiyan, "Computational assessment of Nano-particulate (Al₂O₃/Water) utilization for enhancement of heat transfer with varying straight section lengths in a serpentine tube heat exchanger," *Therm. Sci. Eng. Prog.*, vol. 20, p. 100521, 2020, doi: 10.1016/j.tsep.2020.100521.
- [43] K. Ito, T. Takahashi, T. Fujino, and M. Ishikawa, "Influences of Channel Size and Operating Conditions on Fluid Behavior in a MHD Micro Pump for Micro Total Analysis System," *J. Int. Counc. Electr. Eng.*, vol. 4, no. 3, pp. 220–226, 2014, doi: 10.5370/jicce.2014.4.3.220.

Turnitin Report

Paper ID: 22779:36786754


Sources Overview 

5%
OVERALL SIMILARITY

0 
Flags

5%
Overall Similarity

0%
AI



1	Rumman Hossain, A... CROSSREF	<1%
2	www.researchgate.n... INTERNET	<1%
3	Dhaka University of ... SUBMITTED WORKS	<1%
4	www.laujet.com INTERNET	<1%
5	dspace.daffodilvars... INTERNET	<1%
6	islamicuniversity on ... SUBMITTED WORKS	<1%
7	umpir.ump.edu.my INTERNET	<1%
8	Kabeel, A.E., Emad ... CROSSREF	<1%
9	prism.ucalgary.ca INTERNET	<1%